Matrix Pencil Method for Estimating Parameters of Exponentially Damped/Undamped Sinusoids in Noise

YINGBO HUA, MEMBER, IEEE, AND TAPAN K. SARKAR, SENIOR MEMBER, IEEE

Abstract—**We present a study of a matrix pencil method for estimating parameters (frequencies and damping factors) of exponentially damped and/or undamped sinusoids in noise. Comparison of this method to a polynomial method (SVD-Prony method) shows that the matrix pencil method and the polynomial method are two special cases of a matrix prediction approach but the pencil method is more efficient in computation and less restrictive about signal poles. It is found through perturbation analysis and simulation that, for signals with unknown damping factors, the pencil method is less sensitive to noise than the polynomial method. In Appendix A, a new expression of the Cramer–Rao bound for the exponential signals is presented.**

I. Introduction

We study a matrix pencil method for estimating signal parameters from a noisy exponential data sequence which can be described by

$$y_k = x_k + n_k$$
$$= \Sigma_{i=1,M} |b_i| \exp((\alpha_i + jw_i)k + j\phi_i) + n_k \quad (1.1)$$

$k = 0, 1, \cdots, N-1$. n_k's are the noise. $|b_i|$'s and ϕ_i's are the amplitudes and the phases, respectively. α_i's and w_i's are the damping factors and the frequencies, respectively. M is the number of sinusoids. We also write

$$b_i = |b_i| \exp(j\phi_i) \quad (1.2)$$

$$z_i = \exp(\alpha_i + jw_i). \quad (1.3)$$

The estimation of b_i's can easily be formulated into a linear least square problem if all other parameters are known. M can be estimated by singular value decomposition (SVD) as proposed in [1] and [2]. We, in this paper, address the estimation of the poles z_i's.

Besides the iterative maximum likelihood (ML) or least squares method as in [6] and [7], another well-known approach to the above estimation problem is the polynomial or linear prediction method as in [1]–[5]. The matrix pencil method (or the pencil method) to be presented here represents an alternative approach which exploits the structure of a matrix pencil of the (noiseless) underlying signal x_k, instead of the structure of prediction equations satisfied by x_k.

The idea of using the property of pencil for system identification and spectrum estimation has been exploited since at least as early as the pencil-of-function approach was proposed in [8]–[10]. Recently, the idea has been explored from different directions and resulted in the ESPRIT algorithms as in [11]–[13] and other versions as in [14], [15], and [29]. The matrix pencil method that we first presented in [16], [32], and [33] and shall present here was developed independently from a closely related work [14], [15], [29] by Ouibrahim *et al.* Our matrix pencil method was initially suggested by Hua's insight into the pencil-of-function method; [8], [9] by Jain *et al.*; the ESPRIT [11], [12] by Roy *et al.*; and the SVD-Prony method [1], [2] by Kumaresan and Tufts. It just turns out that a moving window approach is inherent in both Ouibrahim's work [14], [15], [29] and Hua–Sarkar's work [16], [32], [33]. But in contrast to the work by Ouibrahim *et al.*, our matrix pencil method exploits to a greater extend the free-moving window length, which shall be referred to as the pencil parameter. As we shall show, a proper choice of the pencil parameter results in significant improvement in noise sensitivity over Ouibrahim's technique.

In the polynomial method, there is also a free parameter often called polynomial degree (or prediction order). The free polynomial degree and the free pencil parameter bear interesting similarities as will be seen. The role played by the free polynomial degree has been studied before in [1], [2], [4], [5], and [17] as well as in [26] and [28] where the free polynomial degree represents the size of subarrays in the context of wave direction finding.

As one will see, the significance of the pencil parameter is just like the polynomial degree.

We should note that during the review period of two years of this manuscript, several other versions of the matrix pencil method have been found (or recovered), which include the state-space method [25], TLS-ESPRIT [30], and Pro-ESPRIT [31]. Our study of these versions is available in [34]. A fundamental result from [34] is that all those matrix pencil based methods are equivalent to the first-order approximation, and therefore the perturbation analysis presented in this paper holds for all the above-mentioned methods.

Manuscript received October 26, 1987; revised June 26, 1989. This work was supported in part by Aeritalia Corporation and by the Office of Naval Research under Contract N00014-79-C-0598.

The authors are with the Department of Electrical and Computer Engineering, Syracuse University, Syracuse, NY 13244-1240.

IEEE Log Number 9034426.

0096-3518/90/0500-0814$01.00

The objective of this paper is to compare the matrix pencil method originally presented in [16], [32], and [33] to the polynomial method presented in [1] and [2]. Our comparison will show that the pencil method and the polynomial method are two special cases of a matrix prediction approach, but the pencil method is more efficient in computation and less restrictive about the signal poles. It will also be shown by perturbation analysis and simulation that the pencil method is less sensitive to noise than the polynomial method.

In Section II, the pencil method is described. A relationship between the pencil method and the polynomial method is discussed in Section III. A first-order perturbation analysis is provided in Section IV. Some simulation results are given in Section V. In Appendix A, a new expression of the Cramer–Rao bound for exponentially damped sinusoids is presented, which reveals clearly several Cramer–Rao bound properties similar to the corresponding properties of both the polynomial method and the matrix pencil method.

II. Matrix Pencil Method

Like the polynomial method, the matrix pencil method is based on the property of the underlying signal. One property of the exponential signals can be described by Theorem 2.1.

Define

$$\boldsymbol{x}_t = [x_t, x_{t+1}, \cdots, x_{N-L+t-1}]^T. \tag{2.1}$$

(The superscript "T" denotes the transpose.)

$$\underset{(N-L)\times L}{X_0} = [\boldsymbol{x}_{L-1}, \boldsymbol{x}_{L-2}, \cdots, \boldsymbol{x}_0] \tag{2.2}$$

$$\underset{(N-L)\times L}{X_1} = [\boldsymbol{x}_L, \boldsymbol{x}_{L-1}, \cdots, \boldsymbol{x}_1] \tag{2.3}$$

where L is called the pencil parameter, then for part a):

$$X_0 = Z_L B Z_R \tag{2.4}$$

$$X_1 = Z_L B Z Z_R \tag{2.5}$$

where

$$Z_L = \begin{bmatrix} 1 & \cdots & 1 \\ z_1 & \cdots & z_M \\ & \cdots & \\ z_1^{N-L-1} & \cdots & z_M^{N-L-1} \end{bmatrix} \tag{2.6}$$

$$B = \operatorname{diag}\{b_1, b_2, \cdots, b_M\} \tag{2.7}$$

$$Z_R = \begin{bmatrix} z_1^{L-1} & z_1^{L-2} & \cdots & 1 \\ & & \cdots & \\ & & \cdots & \\ z_M^{L-1} & z_M^{L-2} & \cdots & 1 \end{bmatrix} \tag{2.8}$$

$$Z = \operatorname{diag}\{z_1, z_2, \cdots, z_M\}. \tag{2.9}$$

b) Each of $\{z_t;\ t = 1, \cdots, M\}$ is a rank reducing number of the matrix pencil $X_1 - zX_0$ if $M \le L \le N - M$. None of $\{z_t;\ t = 1, \cdots, M\}$ is a rank reducing number of the pencil if $L < M$ or $L > N - M$.

c) If $M \le L \le N - M$, the solutions to the singular generalized eigenvalue problem (the "singular" is due to the fact that X_0 and X_1 do not have full rank for $M < L < N - M$):

$$(X_1 - zX_0)\boldsymbol{q} = 0 \tag{2.10}$$

$$\boldsymbol{p}^H(X_1 - zX_0) = 0 \tag{2.11}$$

subject to $\boldsymbol{q} \in R(X_0^H)$, which denotes the column space of X_0^H, and $\boldsymbol{p} \in R(X_0)$, are

$$\begin{aligned} z &= z_t \\ \boldsymbol{q} &= \boldsymbol{q}_t = \left(t\text{th column of } Z_R^+ = Z_R^H(Z_R Z_R^H)^{-1}\right) \\ \boldsymbol{p}^H &= \boldsymbol{p}_t^H = \left(t\text{th row of } Z_L^+ = (Z_L^H Z_L)^{-1} Z_L^H\right) \end{aligned} \tag{2.12}$$

$t = 1, 2, \cdots, M$. $\boldsymbol{q}_t$ and $\boldsymbol{p}_t$ are called, respectively, the right and the left generalized eigenvectors associated with the generalized eigenvalue z_t. The superscript "+" denotes the Moore-Penrose inverse or pseudoinverse. "H" denotes the conjugate transpose. "-1" denotes the inverse.

Proof: Part a) is easy to verify by substituting (2.6)–(2.9) into (2.4) and (2.5). To show part b), we notice

$$X_1 - zX_0 = Z_L B(Z - zI_M)Z_R$$

where I_M is the $M \times M$ identity matrix, and B and Z are full rank $M \times M$ diagonal matrices. If $z = z_t$, then $(Z - zI_M)_{t,t} = 0$ and the tth column of Z_L and the tth row of Z_R are annihilated in the above expression. If $M \le L \le N - M$, each of Z_L and Z_R has rank M and, therefore, Rank $(X_1 - z_t X_0) + 1 = M =$ Rank $(X_1 - zX_0)$ for z not belonging to $\{z_t;\ t = 1, \cdots, M\}$. If $L < M$, then Rank $(Z_R) = L$ and Rank $((Z - z_t I_M)Z_R) =$ Rank $((Z - zI_M)Z_R) = L$, which implies that Rank $(X_1 - zX_0)$ does not decrease at $z = z_t$. If $L > N - M$, then Rank $(Z_L) = N - L$ and Rank $(Z_L B(Z - z_t I_M)) =$ Rank $(Z_L B(Z - zI_M)) = N - L$, which implies that Rank $(X_1 - zX_0)$ does not decrease at $z = z_t$. Part c) can easily be shown by noticing

$$Z_R Z_R^+ = I_M$$

$$Z_L^+ Z_L = I_M.$$

Since the rank of $X_1 - zX_0$ decreases only at $z = z_t$ and only by one at $z = z_t$, the solutions to (2.10) and (2.11) are unique. (The eigenvectors are unique within a scalar factor.) ∎

This theorem provides the foundation for the matrix pencil method. In the sequel, we shall assume $M \le L \le N - M$ unless otherwise indicated. Based on (2.10) and (2.11), we have the following discussion for computing $\{z_t;\ t = 1, \cdots, M\}$ from X_0 and X_1. Left multiplying (2.10) by X_0^+ yields

$$\begin{aligned} X_0^+ X_1 \boldsymbol{q}_t &= z_t X_0^+ X_0 \boldsymbol{q}_t \\ &= z_t \boldsymbol{q}_t. \end{aligned} \tag{2.13}$$

($X_0^+ X_0$ is the orthogonal projection onto $R(X_0^H)$.) This implies that $\{z_t; t = 1, \cdots, M\}$ are M eigenvalues of $X_0^+ X_1$. Since $X_0^+ X_1$ has rank $M \le L$, there are also $L - M$ zero eigenvalues for the matrix product. Similarly, we can show that $X_1 X_0^+$ has M eigenvalues equal to z_t's and $N - L - M$ zero eigenvalues, and $X_1^+ X_0$ (or $X_0 X_1^+$) has M eigenvalues equal to z_t^{-1}'s and $L - M$ (or $N - L - M$) zero eigenvalues. For the noisy data y_k, we define $\boldsymbol{y}_t$, Y_0, and Y_1 the same way as for $\boldsymbol{x}_t$, X_0, and X_1, respectively, and replace (approximate) the pseudoinverse X_0^+ or X_1^+, by the rank-M truncated pseudoinverse Y_0^+ or Y_1^+, respectively. Y_0^+ is defined as

$$\begin{aligned} Y_0^+ &= \Sigma_{t=1,M}(1/\sigma_{0t})\boldsymbol{v}_{0t}\boldsymbol{u}_{0t}^H \\ &= V_0 A^{-1} U_0^H \end{aligned} \tag{2.14}$$

where $\{\sigma_{0t}; t = 1, \cdots, M\}$ are the M largest singular values of Y_0; $\boldsymbol{v}_{0t}$'s and $\boldsymbol{u}_{0t}$'s are the corresponding singular vectors; $V_0 = [\boldsymbol{v}_{01}, \cdots, \boldsymbol{v}_{0M}]$; $U_0 = [\boldsymbol{u}_{01}, \cdots, \boldsymbol{u}_{0M}]$; and $A = \text{diag}\{\sigma_{01}, \cdots, \sigma_{0M}\}$. Y_1^+ is defined similarly. Note that we use the superscript "+" to denote the (rank-M) pseudoinverse of a rank-M noiseless matrix and the (rank-M) truncated pseudoinverse of a noisy matrix (i.e., a rank-M matrix perturbed by noise). With respect to the noise components in Y_0, the continuity of each element of the truncated pseudoinverse Y_0^+ is preserved at the point where the noise is zero, and so does the continuity of the estimates of z_t's. That is opposed to the fact that the (true) pseudoinverse of Y_0 is discontinuous at the point where the noise is zero, and hence computing the (true) pseudoinverse would face severe numerical problem when the noise level is low. Also note that Y_0^+ is equal to X_0^+ if and only if the noise is zero. Since $Y_0^+ Y_1$ has $L - M$ zero eigenvalues which contain no information about z_t's, its size can be reduced before the eigenvalues are evaluated. Replacing X_0 and X_1 in (2.13) by Y_0 and Y_1, respectively, and substituting (2.14) into (2.13) for Y_0^+ yield

$$V_0 A^{-1} U_0^H Y_1 \boldsymbol{q}_t = z_t \boldsymbol{q}_t. \tag{2.15}$$

Since $V_0^H V_0 = I_M$ and $\boldsymbol{q}_t = V_0 V_0^H \boldsymbol{q}_t$, left multiplying (2.15) by V_0^H yields

$$A^{-1} U_0^H Y_1 V_0 (V_0^H \boldsymbol{q}_t) = z_t (V_0^H \boldsymbol{q}_t). \tag{2.16}$$

Now it can be seen that the estimates of z_t's can be found by computing the eigenvalues of the $M \times M$ nonsymmetrical matrix:

$$Z_E = A^{-1} U_0^H Y_1 V_0. \tag{2.17}$$

Note that the M eigenvalues of Z_E are the same as the M nonzero eigenvalues of $Y_0^+ Y_1$.

Compared to the polynomial method in [1] and [2] which requires SVD of an $(N - L) \times L$ data matrix (for the polynomial method, L represents the degree of polynomial) and finding L roots of an L-degree polynomial, the matrix pencil algorithm, which requires SVD of an $(N - L) \times L$ data matrix and computing M eigenvalues of an $M \times M$ matrix, is certainly more efficient in computation. Like the degree of polynomial, the pencil parameter also plays an important role in reducing noise sensitivity as will be shown later. Unlike the polynomial method which requires all poles to be inside (or outside) the unit circle so that the extraneous $L - M$ poles can be separated from the desired poles, the pencil method is free from such restriction (that is, the pencil method is less restrictive about the signal poles). It is noted that the modification in [4] has removed this restriction by solving for L roots of each of two (forward and backward) L-degree polynomials.

For undamped signals, i.e., $|z_t| = 1$ for all t, it can be shown similarly that $\{z_t; t = 1, \cdots, M\}$ are the rank reducing numbers of the forward-and-backward (FB) matrix pencil:

$$X_{1FB} - zX_{0FB} = \begin{bmatrix} \boldsymbol{x}_L & \boldsymbol{x}_{L-1} & \cdots & \boldsymbol{x}_1 \\ \boldsymbol{x}_0^* & \boldsymbol{x}_1^* & \cdots & \boldsymbol{x}_{L-1}^* \end{bmatrix} - z \begin{bmatrix} \boldsymbol{x}_{L-1} & \boldsymbol{x}_{L-2} & \cdots & \boldsymbol{x}_0 \\ \boldsymbol{x}_1^* & \boldsymbol{x}_2^* & \cdots & \boldsymbol{x}_L^* \end{bmatrix} \tag{2.18}$$

where "*" denotes the conjugate. It can be seen that the whole discussions in this section are also applicable to the FB matrix pencil. But it should be noted that in addition to the condition $M \le L \le N - M$ which is for the pencil to yield the desired eigenvalues, for $M/2 \le L < M$, the FB matrix pencil also yields the desired eigenvalues at z_t's for "almost" all sinusoidal signals. This is because when $M/2 \le L < M$, the two matrices X_{1FB} and X_{0FB} have rank M for "almost" all sinusoidal signals, which can be shown by the approach in [17]. The FB matrix pencil method is in fact the counterpart of the FB polynomial method [1], [28]. Hence, it can be expected that the FB matrix pencil is more robust to noise than the F-only (or B-only) matrix pencil if the signal poles are known to be on the unit circle.

The FB matrix pencil first appeared in [33] and [29]. But in [29], L was fixed to be M.

III. Matrix Prediction Equation

Let us consider the matrix pencil $X_0 - zX_1$. We have known that the generalized eigenvalues (i.e., z_t^{-1} for $t = 1, \cdots, M$) of the pencil are the same as the eigenvalues of the matrix:

$$\begin{aligned} C_1 &= X_1^+ X_0 \\ &= [X_1^+ \boldsymbol{x}_{L-1}\ X_1^+ \boldsymbol{x}_{L-2} \cdots X_1^+ \boldsymbol{x}_0]. \end{aligned} \tag{3.1}$$

It is clear from (3.1) that the tth column of C_1 is simply the minimum norm solution to the equation:

$$X_1 \boldsymbol{a}_t = \boldsymbol{x}_{L-t}. \tag{3.2}$$

However, the vector with its tth element equal to one and all other elements equal to zero is also a solution to (3.2). Replacing the tth column of C_1 by this vector for $t = 1$,

$\cdots, L-1$ yields a new matrix:

$$C_2 = \begin{bmatrix} 0 & 0 & \cdots & 0 & -a_L \\ 1 & & & & -a_{L-1} \\ & 1 & & & \\ & & \ddots & & \vdots \\ & & & 1 & -a_1 \end{bmatrix} \quad (3.3)$$

where the last column is the same as that of C_1, i.e.,

$$\begin{aligned} \boldsymbol{a}_L &= -[a_L\ a_{L-1} \cdots a_1]^T \\ &= X_1^+ \boldsymbol{x}_0. \end{aligned} \quad (3.4)$$

As one can see, $\boldsymbol{a}_L$ is the minimum norm coefficient vector of an L-order backward linear prediction filter ($x_j = -\Sigma_{i=1,L}\, a_i x_{j+i}$ for $j = 0, \cdots, N-L-1$). It is known that the eigenvalues of the new matrix (companion matrix) C_2 are the same as the roots of the L-degree polynomial:

$$1 + \Sigma_{i=1,L} a_i z^{-i}$$

which has M roots at $\{z_i^{-1}; i = 1, \cdots, M\}$ and $L - M$ extraneous nonzero roots with magnitudes less than one [2]. Therefore, the difference between the two methods simply lies in the choice of the solution to (3.2). In other words, C_1 and C_2 are two special solutions to what we call the matrix prediction equation:

$$X_1 C = X_0 \quad (3.5)$$

where $C = [\boldsymbol{a}_1 \cdots \boldsymbol{a}_L]$. Now we show Theorem 3.1.

Theorem 3.1: As long as C is a solution to (3.5), $\{z_i^{-1}; i = 1, \cdots, M\}$ are M eigenvalues of the $L \times L$ matrix C.

Proof: Since Rank $(X_0 - zX_1)$ decreases by one at z_i^{-1} and $X_1(C - zI_L) = X_0 - zX_1$, Rank $(C - zI_L)$ decreases by one at z_i^{-1}. ∎

Similarly, if C is a solution to the "forward" matrix prediction equation $X_0 C = X_1$, then z_i's are M eigenvalues of C. Note that C_1 is a minimum rank (M) and minimum (Frobenius) norm solution to (3.5) while C_2 has the maximum rank L. If $L = M$, the solution to (3.5) is unique so that $C_1 = C_2$, which implies that the pencil method and the polynomial method are equivalent when $L = M$ (note that the above discussion can similarly be carried out for noisy data).

IV. Analysis of Noise Sensitivity

We now present a first-order perturbation analysis of the matrix pencil method with comparison to the polynomial method.

Since the perturbation variance is bounded by the Cramer–Rao bound, a brief discussion of the C-R bound is provided in Appendix A, where a new expression of the C-R bound is presented to reveal several C-R bound properties similar to the corresponding properties of both the polynomial method and the pencil method.

From Section II, we know that the estimated poles obtained by the matrix pencil method are the nonzero eigenvalues of $Y_0^+ Y_1$. (It can easily be shown that $Y_1 Y_0^+$, $Y_0^+ Y_0$, and $Y_0 Y_1^+$ yield the same estimated poles.) It is known from perturbation theory that the perturbation in the eigenvalues (z_i's) due to perturbation in the $Y_0^+ Y_1$ can be written as

$$\delta z_i = \frac{\boldsymbol{p}_i'^H \delta(Y_0^+ Y_1) \boldsymbol{q}_i'}{\boldsymbol{p}_i'^H \boldsymbol{q}_i'} \quad (4.1)$$

where "δ" denotes the first-order differential operator; and $\boldsymbol{p}_i'$ and $\boldsymbol{q}_i'$ are the left and right eigenvectors of $X_0^+ X_1$, i.e.,

$$\boldsymbol{p}_i'^H X_0^+ X_1 = z_i \boldsymbol{p}_i'^H \quad (4.2)$$

$$X_0^+ X_1 \boldsymbol{q}_i' = z_i \boldsymbol{q}_i'. \quad (4.3)$$

Using (2.4) and (2.5), we have $X_0^+ X_1 = Z_R^+ Z Z_R$. Therefore, $\boldsymbol{p}_i'^H$ is the ith row of Z_R, $\boldsymbol{q}_i'$ is the ith column of Z_R^+, and $\boldsymbol{p}_i'^H \boldsymbol{q}_i' = 1$. Because of (2.12), $\boldsymbol{q}_i' = \boldsymbol{q}_i$. Following the approach used in [17] (see equation (13) in [17]) for differentiating the truncated pseudoinverse, we obtain from (4.1)

$$\begin{aligned} \delta z_i &= \boldsymbol{p}_i'^H \big(\delta(Y_0^+) X_1 + X_0 \delta Y_1\big) \boldsymbol{q}_i \\ &= -\boldsymbol{p}_i'^H X_0^+ \delta Y_0 X_0^+ X_1 \boldsymbol{q}_i + \boldsymbol{p}_i'^H X_0^+ \delta Y_1 \boldsymbol{q}_i \\ &= -\boldsymbol{p}_i'^H X_0^+ \delta Y_0 z_i \boldsymbol{q}_i + \boldsymbol{p}_i'^H X_0^+ \delta Y_1 \boldsymbol{q}_i. \end{aligned} \quad (4.4)$$

Here we directly use the perturbation in the truncated pseudoinverse Y_0^+ in terms of the perturbation in the data matrix Y_0, without finding the perturbations in singular values and singular vectors. In the above sense, our approach is neater than the approach in [19] which is based on the perturbation analysis of the intermediate quantities: singular values and singular vectors, and on the condition that the singular values of Y_0 are distinct. Using (2.4) and (2.12), we can show [17], [18]

$$\boldsymbol{p}_i'^H X_0^+ = \boldsymbol{p}_i'^H Z_R^+ B^{-1} Z_L^+ = 1/b_i \boldsymbol{p}_i^H. \quad (4.5)$$

Combining (4.4) and (4.5) yields

$$\delta z_i = 1/b_i \boldsymbol{p}_i^H (\delta Y_1 - z_i \delta Y_0) \boldsymbol{q}_i. \quad (4.6)$$

Note that δY_1 and δY_0 consist of noise components only, i.e.,

$$\delta Y_1 = \begin{bmatrix} n_1 & n_2 & \cdots & n_L \\ & & \cdots & \\ n_{N-L} & n_{N-L+1} & \cdots & n_{N-1} \end{bmatrix} \quad (4.7)$$

$$\delta Y_0 = \begin{bmatrix} n_0 & n_1 & \cdots & n_{L-1} \\ & & \cdots & \\ n_{N-L-1} & n_{N-L} & \cdots & n_{N-2} \end{bmatrix}. \quad (4.8)$$

Some algebraic manipulation of (4.6) yields

$$\delta z_i = (1/b_i) \boldsymbol{q}_i^T P_i^H \boldsymbol{n} \quad (4.9)$$

where

$$\boldsymbol{n} = [n_0 \;\; n_1 \;\; \cdots \;\; n_{N-1}]^T \tag{4.10}$$

$$\underset{N \times L}{P_t} = \begin{bmatrix} 0 & \cdots & 0 \\ & & p_{t,1} \\ p_{t,1} & \vdots & \vdots \\ \vdots & \vdots & p_{t,N-L} \\ p_{t,N-L} & & \end{bmatrix} - z_t^* \begin{bmatrix} & & p_{t,1} \\ p_{t,1} & \vdots & \vdots \\ \vdots & \vdots & p_{t,N-L} \\ p_{t,N-L} & & \\ 0 & \cdots & 0 \end{bmatrix} \tag{4.11}$$

where $p_{t,j}$ is the jth element of $\boldsymbol{p}_t$. If the *FB* matrix pencil is used for undamped signal, then we can show [18] that the perturbation in the estimated z_t is

$$\delta z_{t,FB} = 1/|b_t| [\boldsymbol{q}_t^T P_{t,F}^H \boldsymbol{n} + \boldsymbol{q}_t^T P_{t,B}^H P \boldsymbol{n}^*] \tag{4.12}$$

where the subscript "*FB*" indicates that the estimate is obtained by an *FB* version; $P_{t,F}$ and $P_{t,B}$ are defined the same way as for P_t with $p_{t,j}$ replaced by $p_{t,FB,j}$ and $p_{t,FB,N-L+j}$ respectively; $p_{t,FB,j}$ ($j = 1, 2, \cdots, 2(N - L)$) is the jth element of $\boldsymbol{p}_{t,FB}$; $\boldsymbol{p}_{t,FB}^H$ is the tth row of $Z_{L,FB}^+$;

$$Z_{L,FB} = \begin{bmatrix} \exp(j\phi_1) & \cdots & \exp(j\phi_M) \\ & \cdots & \\ z_1^{N-L-1}\exp(j\phi_1) & \cdots & z_M^{N-L-1}\exp(j\phi_M) \\ z_1^{-L}\exp(-j\phi_1) & \cdots & z_M^{-L}\exp(-j\phi_M) \\ & \cdots & \\ z_1^{-(N-1)}\exp(-j\phi_1) & \cdots & z_M^{-(N-1)}\exp(-j\phi_M) \end{bmatrix} \tag{4.13}$$

and P is the $(N \times N)$ order reversing permutation matrix, i.e.,

$$P = \begin{bmatrix} & & 1 \\ & \cdot^{\cdot^{\cdot}} & \\ 1 & & \end{bmatrix}. \tag{4.14}$$

Now we have obtained δz_t and $\delta z_{t,FB}$ explicitly in terms of the noise vector $\boldsymbol{n}$. If the covariance matrix of the noise vector is known, the first-order perturbation variances in the estimated z_t, w_t, and α_t can straightforward be found from (4.9) or (4.12) (at least by numerical computation) for any given signal. For example, we can write, from (4.9)

$$\text{Var}(\delta z_t) = (1/|b_t|^2)\boldsymbol{q}_t^T P_t^H R_{nn} P_t \boldsymbol{q}_t^* \tag{4.15}$$

where R_{nn} is the covariance matrix of $\boldsymbol{n}$. To evaluate the perturbation variance, we will let

$$E\{\boldsymbol{n}\} = 0$$
$$E\{\boldsymbol{n}\boldsymbol{n}^T\} = 0$$
$$E\{\boldsymbol{n}\boldsymbol{n}^H\} = R_{nn} = 2\sigma^2 I_N$$

where $E\{\;\}$ denotes the expectation, and $2\sigma^2$ the noise variance.

A. Simple Case Study

Simplified expression of the perturbation variance for one undamped sinusoid can be obtained as follows.

One Complex Sinusoid: Assume that $x_k = b_1 \exp(jw_1 k)$. Then we can show [18] that

$$\text{Var}(\delta w_1)_{\text{pencil}} = 1/2\,\text{Var}(\delta z_1)_{\text{pencil}} = \frac{1}{\text{SNR}_1}\begin{cases} \dfrac{1}{(N-L)^2 L} & \text{for } L \le N/2 \\ \dfrac{1}{(N-L)L^2} & \text{for } L \ge N/2 \end{cases} \tag{4.16}$$

for the matrix pencil method, and

$$\text{Var}(\delta w_1)_{\text{poly}} = 1/2\,\text{Var}(\delta z_1)_{\text{poly}} = \frac{1}{\text{SNR}_1}\begin{cases} \dfrac{2(2L+1)}{3(N-L)^2 L(L+1)} & \text{for } L \le N/2 \\ \dfrac{2(-(N-L)^2 + 3L^2 + 3L + 1)}{3(N-L)L^2(L+1)^2} & \text{for } L \ge N/2 \end{cases} \tag{4.17}$$

for the (either forward or backward) polynomial method. $\mathrm{SNR}_1 = |b_1|^2/2\sigma^2$. Since the analytical results (including those presented later) are obtained through the first-order approximation, they are valid only when SNR_1 is very large. However, based on our simulations, those results are good approximations if $\mathrm{SNR}_1 \geq 30$ dB, or more precisely, if SNR_1 is above threshold. Note that L in (4.17) represents the polynomial degree for the polynomial method.

It is easy to observe from (4.16) that the pencil method is the most sensitive to noise when the free pencil parameter is equal to M or $N - M$. $N/3$ and $2N/3$ are the best choices for L. In fact, all values satisfying $N/3 \leq L \leq 2N/3$ appear to be good choices in general. This phenomenon can be seen in all other cases.

We should mention that a first-order perturbation analysis of the polynomial method has also been presented in [20] where the result only for single sinusoid is obtained. Unfortunately, we found that their result (equation (31) in [20]) is not consistent with (4.17) for $L \geq N/2$ (in fact, equation (31) in [20] is not consistent by itself when $M = L - M$, i.e., $L = N/2$ in our notation).

With (4.16) and (4.17), it can be shown that

$$\mathrm{Var}\,(\delta w_1)_{\text{pencil}} \leq \mathrm{Var}\,(\delta w_1)_{\text{poly}} \tag{4.18}$$

with equality only when $L = 1$ (i.e., $L = M$).

It is interesting, however, that if the *FB* versions of the pencil and polynomial methods are used, then we can show [18] that

$$\begin{aligned}\mathrm{Var}\,(\delta z_{1,FB})_{\text{pencil}} &= \mathrm{Var}\,(\delta w_{1,FB})_{\text{pencil}}\\ &= \frac{1}{\mathrm{SNR}_1}\begin{bmatrix}\dfrac{1}{L(N-L)^2} & \text{for } L \leq N/2\\ \dfrac{1}{L^2(N-L)} & \text{for } L \geq N/2\end{bmatrix}\end{aligned} \tag{4.19}$$

and

$$\begin{aligned}\mathrm{Var}\,(\delta z_{1,FB})_{\text{poly}} &\geq \mathrm{Var}\,(\delta w_{1,FB})_{\text{poly}}\\ &= \frac{1}{\mathrm{SNR}_1}\begin{bmatrix}\dfrac{1}{L(N-L)^2} & \text{for } L \leq N/2\\ \dfrac{1}{L^2(N-L)} & \text{for } L \geq N/2.\end{bmatrix}\end{aligned} \tag{4.20}$$

The first equality in (4.20) holds only when $L = 1$ (i.e., $L = M$ [17]). The above two equations indicate that the *FB* versions of the two methods have very close noise sensitivity with respect to the estimated frequencies.

The Cramer–Rao bound for $\mathrm{Var}\,(w_1)$ or $\mathrm{Var}\,(w_{1,FB})$ is known [24] to be

$$\mathrm{CRB} = (1/\mathrm{SNR}_1)6/N(N^2-1). \tag{4.21}$$

From (4.16), (4.19), and (4.20), we know

$$\begin{aligned}&\mathrm{Min}_L\ \mathrm{Var}\,(\delta w_1)_{\text{pencil}}\\ &= \mathrm{Min}_L\ \mathrm{Var}\,(\delta w_{1,FB})_{\text{pencil}}\\ &= \mathrm{Min}_L\ \mathrm{Var}\,(\delta w_{1,FB})_{\text{poly}}\\ &= \mathrm{Var}\,(\delta w_{1,FB}) \quad \text{when } L = N/3 \quad \text{or } 2N/3\\ &= (1/\mathrm{SNR}_1)27/4N^3.\end{aligned} \tag{4.22}$$

Note that although this expression is valid only for the case where $N/3$ is an integer, the approximation to be given in (4.24) is true for all $N \geq 3$. Based on (4.21) and (4.22), the efficiency is

$$\text{eff.} = \mathrm{Var}/\mathrm{CRB} = 27N(N^2-1)/24N^3 \geq 1 \tag{4.23}$$

where $N \geq 3$, and the last equality holds only when $N = 3$. Since $N^2 - 1 \approx N^2$, we have

$$\text{eff.} \approx 27/24 = 1.125. \tag{4.24}$$

This result supports the observation that the polynomial method [1], [2], [21] and the matrix pencil [17], [18] method (with optimum choice of L) generally have a good and constant (with respect to N) efficiency.

Two Complex Sinusoids: If we let $x_k = b_1 z_1^k + b_2 z_2^k$, then simplifying the theoretical perturbation variances of δz_i or δw_i has not been successful. But we always can evaluate the theoretical variances numerically with use of the general result given by (4.9) and (4.12). With the parameters defined as: $M = 2$, $N = 25$, $\alpha_1 = -0.01$, $\alpha_2 = -0.02$, $f_1 - f_2 = -0.02$, and any ϕ_1 and ϕ_2, we plotted the theoretical perturbation variances in Fig. 1. This plot ("*") shows

$$10\log_{10}\left(\mathrm{CRB}/\mathrm{Var}\,(\delta f_1)\right) \text{ versus } L$$

for both the polynomial method and the pencil method. Note that $f_i = w_i/2\pi$, and the CRB in the above expression denotes the C-R bound for the two sinuosids, which should not be confused with the CRB in (4.21). Again, it is observed that $\mathrm{Var}\,(\delta f_1)_{\text{pencil}} \leq \mathrm{Var}\,(\delta f_1)_{\text{poly}}$ with equality only when $L = M = 2$. (The variances for the two methods can differ by more than 2 dB.) In fact, this phenomenon has been observed for all choices of signal parameters and especially for weakly damped signals.

As predicted by (4.19) and (4.20), the FB versions (only for undamped signals) do not show noticeable differences of frequency perturbation variances. In other words, the *FB* matrix pencil method and the TK method [1] have almost the same performance with respect to the accuracy of the frequency estimation. (We also found that the frequency perturbation variances for the two *FB* versions are not exactly the same in general [18].) But the *FB* matrix pencil method still has the computational advantage over the *FB* polynomial method (i.e., the Tufts–Kumaresan method [1]).

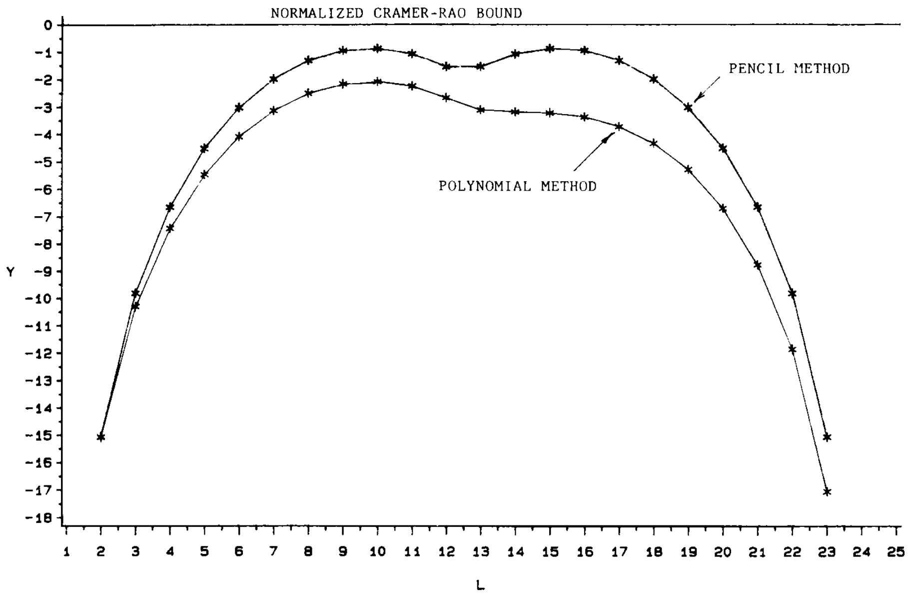

Fig. 1. This plot shows $10 \log_{10} (\text{CRB}/\text{Var}(\delta f_1))$ versus L where Var (δf_1) ("*") was computed from perturbation analysis. The signal parameters are $M = 2$, $N = 25$, $\alpha_1 = -0.01$, $\alpha_2 = -0.02$, $f_1 - f_2 = -0.02$, and any ϕ_1 and ϕ_2.

B. General Case Study

In this subsection, we present some fundamental properties for the pencil method. All these properties are observed from (4.9) and (4.12) which are for any sinusoidal signal.

Properties Similar for the Polynomial Method:

1) If the signal is undamped sinusoids and $L \leq (N - 1)/2$, the perturbations in z_t or $z_{t,FB}$ due to the noise components, n_k for $L \leq k \leq N - L - 1$, are zero.

2) Var (δz_t) or Var $(\delta z_{t,FB})$ is inversely proportional to $\text{SNR}_t = |b_t|^2/2\sigma^2$, and is independent of SNR_j for j not equal to t.

3) Var (δz_t) is invariant to the phases and the group shift of frequencies.

4) Var $(\delta z_{t,FB})$ is invariant to the group shift of phases and the group shift of frequencies.

Note that the properties 2)–4) are shared by the C-R bound. See Appendix A.

5) Var $(\delta z_t) = 2$ Var $(\delta w_t) = 2$ Var $(\delta \alpha_t)$.

6) For the case where $|z_t| = 1$ for all t, we have

$$\text{Var}(\delta z_{t,FB}) \leq 1/2 \, \text{Var}(\delta z_t) \tag{4.25}$$

with equality if

$$(w_t - w_j)(N - 1) + 2(\phi_t - \phi_j) = 2m\pi \tag{4.26}$$

or

$$w_t - w_j = 2m\pi/(N - L)$$

or

$$N - L \gg 1$$

or

$$M = 1$$

where t is not equal to j, and m is an integer. Equation (4.25) has not been proved completely. But for the detailed discussions, see [18].

Properties Different from the Polynomial Method:

7) Since $Y_1 - zY_0$ and $Y_1^T - zY_0^T$ have the same rank reducing numbers, δz_t is symmetrical about $L = N/2$. This symmetry can be seen from (4.14) and Fig. 1.

8) A unique property of the *FB* matrix pencil method is that the perturbation $\delta \alpha_{t,FB}$ is zero, which implies

$$\text{Var}(\delta w_{t,FB})_{\text{pencil}} = \text{Var}(\delta z_{t,FB})_{\text{pencil}}. \tag{4.27}$$

This is in contrast to

$$\text{Var}(\delta w_{t,FB})_{\text{poly}} = \text{Var}(\delta z_{t,FB})_{\text{poly}} \tag{4.28}$$

with equality only when $L = M$ [17].

9) Due to properties 5) and 8), (4.25) can be replaced by

$$\text{Var}(\delta w_{t,FB})_{\text{pencil}} = \text{Var}(\delta w_t)_{\text{pencil}}.$$

A proof of (4.27) is provided in Appendix B. Equation (4.27) implies that the estimated poles are perturbed by (small) noise along the unit circle only.

V. Simulation Results

To justify our perturbation analysis in Section IV, we did computer simulation. In this simulation, the IMSL software (with VAX/VMS 785 at Syracuse University) was used to generate the white Gaussian noise, to solve

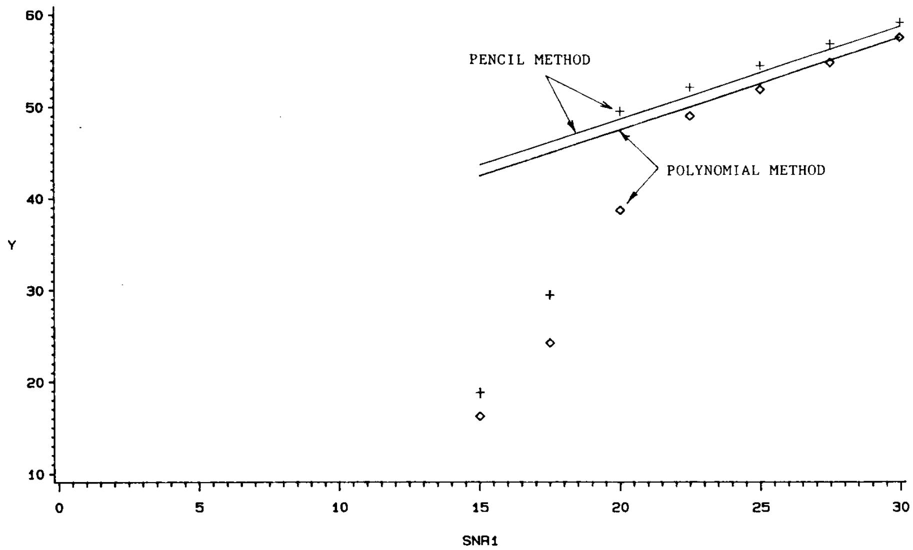

Fig. 2. This plot shows $-10 \log_{10} (\text{Var}(\delta f_1))$ versus SNR_1. The "pluses" are simulation results for the pencil method, and the "diamonds" are for the polynomial method. The straight lines were computed from the perturbation analysis. $L = 10$ (an optimum choice) was chosen. The signal parameters (except $\phi_1 = \phi_2 = 30°$) are the same as for Fig. 1.

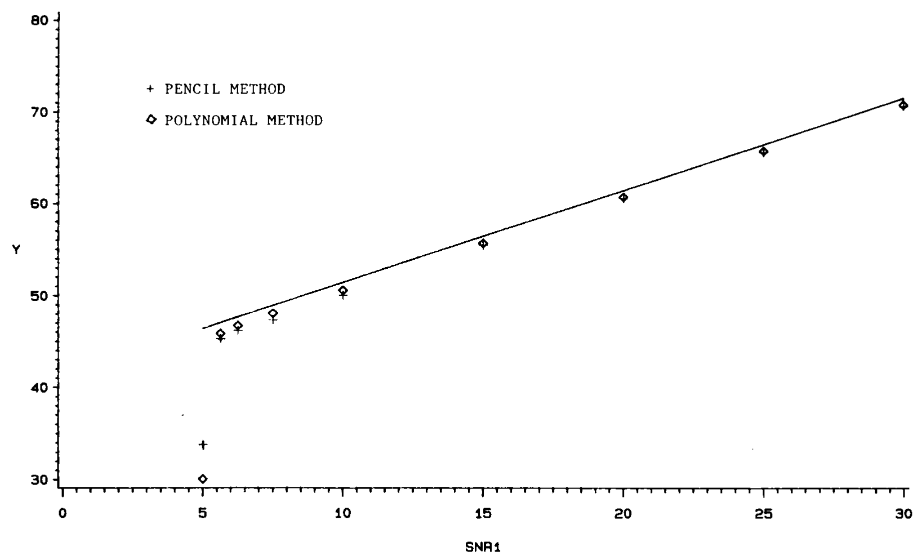

Fig. 3. This plot shows $-10 \log_{10} (\text{Var}(\delta f_{1,FB})$ versus SNR_1. The frequency was estimated by the FB versions of the pencil and polynomial methods with $L = 17$ (an optimum choice). The straight lines, "pluses," and "diamonds" have the same meaning as in Fig. 2. The signal parameters are $M = 2$, $N = 25$, $\alpha_1 = \alpha_2 = 0$, $f_1 = 0.2$, $f_2 = 0.22$, $\phi_2 = 0$, and $\phi_1 = -3.6°$.

the eigenvalue problem as required by the pencil method, and to find the roots of polynomial as required by the polynomial method. Each sample variance was computed based on 200 estimates which were perturbed by 200 independent noise sequences added on x_k, $k = 0, 1, \cdots, N - 1$. For each case or figure, the same (noisy) data were used for both the pencil method and the polynomial method. We first present the case where the signal consists of two sinusoids as given in the previous section. Fig. 2 shows $-10 \log_{10} (\text{Var}(\delta f_1))$ versus SNR_1. $L = 10$ ($\approx N/3$) was used for both of the methods because it is the optimum choice for both of the methods with the

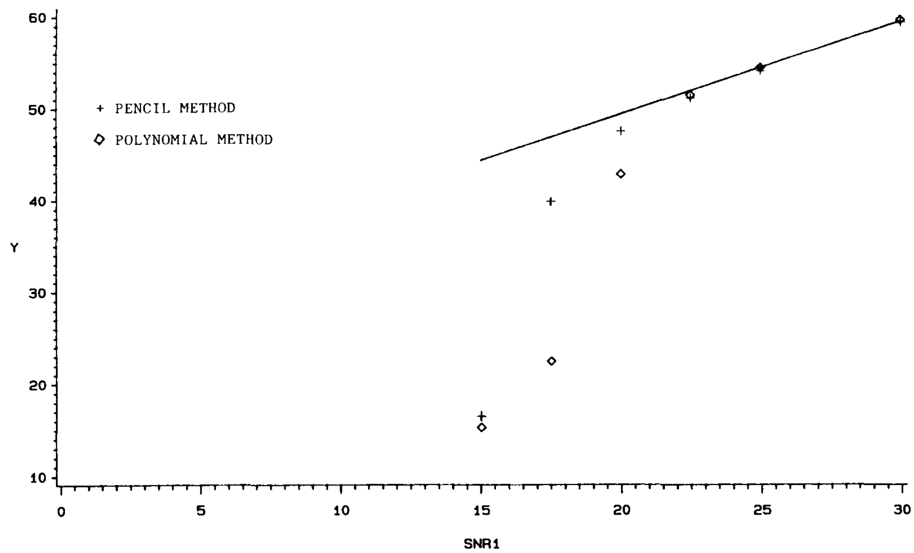

Fig. 4. See Fig. 3. The only difference here is that $\phi_1 = 86.4°$ instead of $-3.6°$.

given signal data (see Fig. 1). The straight lines were computed from (4.9) (assuming the noise is white). The "pluses" are simulation results for the pencil method while the "diamonds" are for the polynomial method. As can be seen, the simulation results are consistent with the perturbation analysis for high SNR (i.e., when SNR is above threshold). Note that the advantage in noise sensitivity of the pencil method over the polynomial method is preserved in the threshold region.

To compare the *FB* versions of the two methods for undamped signals, we chose $M = 2$, $N = 25$, $f_1 = 0.2$, $f_2 = 0.22$, $\alpha_1 = \alpha_2 = 0$, $\phi_2 = 0$, and $\phi_1 = -3.6°$ and $86.4°$, respectively. Figs. 3 and 4 show $-10 \log_{10}$ (Var $(\delta f_{1,FB})$) versus SNR_1 for $\phi_1 = -3.6°$ and $\phi_1 = 86.4°$, respectively. For the two figures, $L = 17$ ($\approx 2N/3$) was used for both of the methods because it is the optimum choice for both of the *FB* versions with the given signal data [17], [18]. As can be seen, the two methods have very close Var $(\delta f_{t,FB})$. In Figs. 3 and 4, we plotted two straight lines (first-order perturbation variances) for the two methods, but they are overlayed in the plot. An important thing that one should observe from the two plots is that both the threshold and the perturbation variance are significantly affected by the phase difference. It can be shown (see [17] and [18]) that $\phi_1 - \phi_2 = -3.6°$ makes X_1 and X_0 the best conditioned, while $\phi_1 - \phi_2 = 86.4°$ makes X_1 and X_0 the worst conditioned. Note that $\phi_1 - \phi_2 = 86.4°$ satisfies (4.24).

VI. Conclusion

We have presented a study of a matrix pencil method with comparison to the polynomial method proposed in [1] and [2]. We have shown that the two methods are two special cases of a matrix prediction approach, but the pencil method is more efficient in computation, less restrictive about signal poles, and less sensitive to noise for signals with unknown damping factors than the polynomial method. The C-R bound has also been discussed in Appendix A in a unique way.

Appendix A

In this appendix, we shall derive a Fisher information matrix which is in such a form that some relations between the Cramer-Rao bound and the signal parameters are easily seen. From (1.1), we can write

$$\boldsymbol{y} = \boldsymbol{x} + \boldsymbol{n} \tag{A.1}$$

where $\boldsymbol{y} = [y_0, y_1, \cdots, y_{N-1}]^T$ and $\boldsymbol{x} = [x_0, x_1, \cdots, x_{N-1}]^T$. If the probability density function (pdf) of $\boldsymbol{n}$ is normal, i.e., $N(\boldsymbol{0}, 2\sigma^2 I_N)$, then the pdf of $\boldsymbol{y}$ is $N(\boldsymbol{x}, 2\sigma^2 I_N)$. It is clear that the mean vector $\boldsymbol{x}$ depends on the parameter vector $\boldsymbol{\theta}$ defined as

$$\boldsymbol{\theta} = [\boldsymbol{\theta}_1^T, \cdots, \boldsymbol{\theta}_M^T]^T \tag{A.2}$$

$$\boldsymbol{\theta}_t = \left[|b_t|, \phi_t, \alpha_t, w_t\right]^T. \tag{A.3}$$

Let θ_t denote the tth element of $\boldsymbol{\theta}$. Then the (t, j)th element of the Fisher information matrix J can be shown to be

$$(J)_{t,j} = 1/\sigma^2 \Sigma_{k=0,N-1} \operatorname{Re}\left\{(dx_k/d\theta_t)(dx_k^*/d\theta_j)\right\} \tag{A.4}$$

where $d(\ )/d\theta_t$ is partial derivative. But J can be partitioned as

$$J = \left\{J_{t,j};\ t, j = 1, 2, \cdots, M\right\} \tag{A.5}$$

where $J_{t,j}$ is a 4×4 (t, j)th block matrix of J, which can be shown from (A.4) to be

$$J_{t,j} = 1/\sigma^2 B_t \operatorname{Re}\left\{\exp\left(j(\phi_t - \phi_j)\right) Z_{t,j}\right\} B_j \tag{A.6}$$

in which

$$B_t = \text{diag}\left\{1, |b_t|, |b_t|, |b_t|\right\} \tag{A.7}$$

$$Z_{t,j} = \begin{bmatrix} \beta_{t,j,0} & -j\beta_{t,j,0} & \beta_{t,j,1} & -j\beta_{t,j,1} \\ j\beta_{t,j,0} & \beta_{t,j,0} & j\beta_{t,j,1} & \beta_{t,j,1} \\ \beta_{t,j,1} & -j\beta_{t,j,1} & \beta_{t,j,2} & -j\beta_{t,j,2} \\ j\beta_{t,j,1} & \beta_{t,j,1} & j\beta_{t,j,2} & \beta_{t,j,2} \end{bmatrix} \tag{A.8}$$

$$\beta_{t,j,0} = \Sigma_{k=0,N-1}(z_t z_j^*)^k \tag{A.9}$$

$$\beta_{t,j,1} = \Sigma_{k=0,N-1}k(z_t z_j^*)^k \tag{A.10}$$

$$\beta_{t,j,2} = \Sigma_{k=0,N-1}k^2(z_t z_j^*)^k. \tag{A.11}$$

It can be seen that β's are invariant to the group shift of frequencies. Furthermore, we can write

$$\begin{aligned} \text{Re}\left\{\exp\left(j(\phi_t - \phi_j)\right)Z_{t,j}\right\} &= \theta_{t,j}X_{t,j} \\ &= X_{t,j}\theta_{t,j} \end{aligned} \tag{A.12}$$

where

$$X_{t,j} = \text{Re}\left\{Z_{t,j}\right\} \tag{A.13}$$

$$\theta_{t,j} = \begin{bmatrix} \theta'_{t,j} & 0 \\ 0 & \theta'_{t,j} \end{bmatrix} \tag{A.14}$$

$$\theta'_{t,j} = \begin{bmatrix} \cos(\phi_t - \phi_j) & \sin(\phi_t - \phi_j) \\ -\sin(\phi_t - \phi_j) & \cos(\phi_t - \phi_j) \end{bmatrix}. \tag{A.15}$$

Note that $\theta_{t,j}\theta_{j,k} = \theta_{t,k}$, $\theta_{t,j}^{-1} = \theta_{t,j}^T = \theta_{j,t}$, and $\theta_{t,t} = I_4$. After substituting (A.12) into (A.6), the 4×4 (t, j)th block matrix of J^{-1} can be shown to be

$$J^{t,j} = \sigma^2 B_t^{-1} X^{t,j}\theta_{t,j}B_j^{-1} \tag{A.16}$$

where $X^{t,j}$ is the 4×4 (t, j)th block matrix of $X^{-1} = \{X_{t,j}\}^{-1}$ (which is independent of $|b_t|$ and ϕ_t). Then the tth diagonal block matrix of J^{-1} is

$$J^{t,t} = \sigma^2 B_t^{-1} X^{t,t} B_t^{-1}. \tag{A.17}$$

Since the 4 diagonal elements of $J^{t,t}$ are the C-R bounds for $|b_t|$, ϕ_t, α_t, and w_t, respectively, the following theorem can easily be shown from (A.17).

Theorem A.1: If the parameters $(|b_t|, \phi_t, \alpha_t, w_t)$ for all t are unknown, then the Cramer–Rao bounds for (ϕ_t, α_t, w_t) are independent of $|b_j|$ for j not equal to t but proportional to $1/|b_t|^2$, the bound for $|b_t|$ is independent of $|b_j|$ for all j, and the bounds for all parameters are independent of phases ϕ_j for all j and the group shift of frequencies.

If α_t's are known (e.g., $\alpha_t = 0$ for all t), the above results are still true except that the C-R bounds depend upon the phases (but not the group shift of phases). This is because a symmetry in (A.8) is destroyed when α_t's are known. The C-R bound has been studied for sinusoidal signals in [22]–[24], and all the properties, except the phase independency when α_i's are unknown, in Theorem A.1 have been known. However, we think that the above formulation of the C-R bound is unique. ■

Appendix B

Here we prove (4.27) with the assumption $|z_t| = 1$ for all t. Since $\delta w_{t,FB} = \text{Im}\{\delta z_{t,FB}/z_t\}$ and $\delta\alpha_{t,FB} = \text{Re}\{\delta z_{t,FB}/z_t\}$, we need to show that $\delta z_{t,FB}/z_t$ is purely imaginary. Similar to δz_t in (4.6), $\delta z_{t,FB}$ can be shown [18] to be

$$\delta z_{t,FB}/z_t = 1/(z_t|b_t|)\boldsymbol{p}_{t,FB}^H(\delta Y_{1,FB} - z_t\delta Y_{0,FB})\boldsymbol{q}_t. \tag{D.1}$$

We can write

$$\boldsymbol{p}_{t,FB}^H = [\boldsymbol{p}_{t,F}^H, \boldsymbol{p}_{t,B}^H] \tag{D.2}$$

$$\delta Y_{1,FB} = \begin{bmatrix} \delta Y_1 \\ \delta Y_{1,b} \end{bmatrix} \tag{D.3}$$

$$\delta Y_{0,FB} = \begin{bmatrix} \delta Y_0 \\ \delta Y_{0,b} \end{bmatrix} \tag{D.4}$$

where $\delta Y_1^* = \delta Y_{0,b}P$ and $\delta Y_0^* = \delta Y_{1,b}P$ [see (2.18)]. Then (D.1) becomes

$$\delta z_{t,FB}/z_t = (1/|b_t|)[T_F + T_B] \tag{D.5}$$

where

$$T_F = 1/z_t\boldsymbol{p}_{t,F}^H(\delta Y_1 - z_t\delta Y_0)\boldsymbol{q}_t \tag{D.6}$$

$$T_B = 1/z_t\boldsymbol{p}_{t,B}^H(\delta Y_{1,b} - z_t\delta Y_{0,b})\boldsymbol{q}_t. \tag{D.7}$$

Since $\boldsymbol{p}_{t,FB}^H$ is the ith row of $Z_{L,FB}^+$ [see (4.13)], it can be shown [18] that

$$\boldsymbol{p}_{t,B}^H = z_t^L\boldsymbol{p}_{t,F}^T. \tag{D.8}$$

Since $Z_R = E_{L-1}Z_R^*P$ [see (2.8)] and

$$E_{L-1} = \text{diag}\left\{z_1^{L-1}, \cdots, z_M^{L-1}\right\}$$

we have

$$\boldsymbol{q}_t = P\boldsymbol{q}_t^* z_t^{-(L-1)}. \tag{D.9}$$

Substituting (D.8) and (D.9) into (D.7) yields

$$T_B = 1/z_t^*\boldsymbol{p}_{t,F}^T(z_t^*\delta Y_{1,b}P - \delta Y_{0,b}P)\boldsymbol{q}_t^*. \tag{D.10}$$

Comparing (D.10) to (D.6) yields

$$T_B = -T_F^* \tag{D.11}$$

which implies

$$\delta z_{t,FB}/z_t = j2\,\text{Im}\left\{T_F\right\}/|b_t|. \tag{D.12}$$ □

Acknowledgment

Encouraged by a constructive comment made by a reviewer of our earlier correspondence [33], we have expanded that correspondence into this paper. The presentation of this work has been greatly helped by the comments of five reviewers.

References

[1] D. W. Tufts and R. Kumaresan, "Estimation of frequencies of multiple sinusoids: Making linear prediction perform like maximum likelihood," *Proc. IEEE*, vol. 70, pp. 975-989, Sept. 1982.

[2] R. Kumaresan and D. Tufts, "Estimating the parameters of exponentially damped sinusoids and pole-zero modeling in noise," *IEEE Trans. Acoust., Speech, Signal Processing*, vol. ASSP-30, pp. 833-840, Dec. 1982.

[3] M. L. Van Blaricum and R. Mittra, "Problems and solutions associated with Prony's method for processing transient data," *IEEE Trans. Antennas Propagat.*, vol. AP-26, pp. 174-182, Jan. 1978.

[4] A. J. Porat and B. Friedlander, "A modification of the Kumaresan-Tufts method for estimating rational impulse response," *IEEE Trans. Acoust., Speech, Signal Processing*, vol. ASSP-34, pp. 1336-1338, Oct. 1986.

[5] M. A. Rahman and K. B. Yu, "Total least squares approach for frequency estimation using linear prediction," *IEEE Trans. Acoust., Speech, Signal Processing*, vol. ASSP-35, pp. 1440-1454, Oct. 1987.

[6] Y. Bresler and A. Macovski, "Exact maximum likelihood parameter estimation of superimposed exponential signals in noise," *IEEE Trans. Acoust., Speech, Signal Processing*, vol. ASSP-34, pp. 1081-1089, Oct. 1986.

[7] R. Kumaresan, L. L. Scharf, and A. K. Shaw, "An algorithm for pole-zero modeling and spectral analysis," *IEEE Trans. Acoust., Speech, Signal Processing*, vol. ASSP-34, pp. 637-640, June 1986.

[8] V. K. Jain, "Filter analysis by use of pencil-of-functions: Part I," *IEEE Trans. Circuits Syst.*, vol. CAS-21, pp. 574-579, Sept. 1974.

[9] —, "Filter analysis by use of pencil-of-functions, Part II," *IEEE Trans. Circuits Syst.*, vol. CAS-21, pp. 580-583, Sept. 1974.

[10] V. K. Jain, T. K. Sarkar, and D. D. Weiner, "Rational modeling by the pencil-of-function method," *IEEE Trans. Acoust., Speech, Signal Processing*, vol. ASSP-31, pp. 564-573, June 1983.

[11] A. Paulraj, R. Roy, and T. Kailath, "Estimation of signal parameters via rotational invariance techniques—ESPRIT," in *Proc. 19th Asilomar Conf. Circuits, Syst., Comput.*, Asilomar, CA, Nov. 1985.

[12] R. Roy, A. Paulraj, and T. Kailath, "ESPRIT—A subspace rotation approach to estimation of parameters of cisoids in noise," *IEEE Trans. Acoust., Speech, Signal Processing*, vol. ASSP-34, pp. 1340-1342, Oct. 1986.

[13] R. H. Roy, "ESPRIT—Estimation of signal parameters via rotational invariance techniques," Ph.D. dissertation, Stanford Univ., Aug. 1987.

[14] H. Ouibrahim, D. D. Weiner, and T. K. Sarkar, "A generalized approach to direction finding," *IEEE Trans. Acoust., Speech, Signal Processing*, vol. ASSP-36, pp. 610-612, Apr. 1988.

[15] H. Ouibrahim, "A generalized approach to direction finding," Ph.D. dissertation, Syracuse Univ., Syracuse, NY, Dec. 1986.

[16] Y. Hua and T. K. Sarkar, "Further analysis of three modern techniques for pole retrieval from data sequence," in *Proc. 30th Midwest Symp. Circuits Syst.*, Syracuse, NY, Aug. 1987.

[17] —, "Perturbation analysis of TK method for harmonic retrieval problems," *IEEE Trans. Acoust., Speech, Signal Processing*, vol. ASSP-36, pp. 228-240, Feb. 1988.

[18] Y. Hua, "On techniques for estimating parameters of exponentially damped/undamped sinusoids in noise," Ph.D. dissertation, Syracuse Univ., 1987.

[19] R. J. Vaccaro and A. C. Kot, "A perturbation theory for the analysis of SVD-based algorithms," in *Proc. ICASSP-87*, Dallas, TX, Apr. 1987.

[20] A. C. Kot, S. Parthasarathy, D. W. Tufts, and R. J. Vaccaro, "The statistical performance of state-variable balancing and Prony's method in parameter estimation," in *Proc. ICASSP-87*, Dallas, TX, Apr. 1987.

[21] B. Porat and B. Friedlander, "On the accuracy of the Kumaresan-Tufts method for estimating complex damped exponentials," *IEEE Trans. Acoust., Speech, Signal Processing*, vol. ASSP-35, pp. 231-235, Feb. 1987.

[22] R. Birgenhier, "Parameter estimation of multiple signals," Ph.D. dissertation, Univ. Calif., Los Angeles, 1972.

[23] D. C. Rife, "Digital tone parameter estimation in the presence of Gaussian noise," Ph.D. dissertation, Polytechnic Inst., Brooklyn, NY, June 1973.

[24] S. W. Lang and J. H. McClellan, "Frequency estimation with maximum entropy spectral estimators," *IEEE Trans. Acoust., Speech, Signal Processing*, vol. ASSP-28, pp. 716-724, Dec. 1980.

[25] S. Y. Kung, K. S. Arun, and D. V. Bhaskar Rao, "State-space and singular value decomposition based approximation method for the harmonic retrieval problem," *J. Opt. Soc. Amer.*, vol. 73, no. 12, Dec. 1983.

[26] T.-J. Shan, M. Wax, and T. Kailath, "On spatial smoothing for direction-of-arrival estimation of coherent signals," *IEEE Trans. Acoust., Speech, Signal Processing*, vol. ASSP-33, pp. 806-811, Aug. 1985.

[27] J. E. Evans, J. R. Johnson, and D. F. Sun, "High resolution angular spectrum estimation techniques for terrain scattering analysis and angle of arrival estimation," in *Proc. 1st ASSP Workshop Spectral Estimation Modeling*, Hamilton, Ont., Canada, 1981, pp. 134-139.

[28] —, "Application of advanced signal processing techniques to angle-of-arrival estimation in ATC navigation and surveillance systems," M.I.T. Lincoln Lab., Tech. Rep. 582, 1982.

[29] H. Ouibrahim, D. D. Weiner, and Z. Y. Wei, "Angle of arrival estimation using a forward-back moving window," in *Proc. 30th Midwest Symp. Circuits Syst.*, Syracuse, NY, Aug. 1987, pp. 563-566.

[30] M. Zoltowski, "Novel techniques for the estimation of array signal parameters based on matrix pencil, subspace rotations and total least squares," in *Proc. IEEE ICASSP-88*, vol. 4, New York, NY, Apr. 1988, pp. 2861-2864.

[31] R. Roy and T. Kailath, "ESPRIT and total least squares," in *Proc. 21st Asilomar Conf. Signals, Syst., Comput.*, Nov. 1987, pp. 297-310.

[32] Y. Hua and T. K. Sarkar, "Matrix pencil method and its performance," in *Proc. ICASSP-88*, Apr. 1988.

[33] —, "A variation of ESPRIT for harmonic retrieval from a finite noisy data sequence," *IEEE Trans. Acoust., Speech, Signal Processing*, submitted for publication.

[34] —, "On SVD for estimating the generalized eigenvalues of singular matrix pencils perturbed by noise," *IEEE Trans. Acoust., Speech Signal Processing*, submitted for publication.

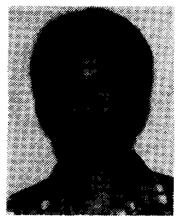

Yingbo Hua (S'86–M'87) was born in Jiangsu, China, on November 26, 1960. He received the B.S. degree in control engineering from Southeastern University (Nanjing Institute of Technology), Nanjing, China, in 1982, and the M.S. and Ph.D. degrees, both in electrical engineering, from Syracuse University, Syracuse, NY, in 1983 and 1988, respectively.

He was a Graduate Teaching Assistant from 1984 to 1985, a Graduate Fellow from 1985 to 1986, a Graduate Research Assistant from 1986 to 1988, and a Research Associate from 1988 to 1989, at Syracuse University. His research interests include transient signal processing, wave direction finding, spectrum estimation, and fast algorithms.

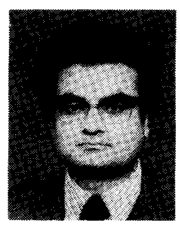

Tapan K. Sarkar (S'69–M'76–SM'81) was born in Calcutta, India, on August 2, 1948. He received the B.Tech. degree from the Indian Institute of Technology, Kharagpur, India, in 1969, the M.Sc.E. degree from the University of New Brunswick, Fredericton, Canada, in 1971, and the M.S. and Ph.D. degrees from Syracuse University, Syracuse, NY, in 1975.

From 1975 to 1976 he was with the TACO Division of General Instruments Corporation. He was with the Rochester Institute of Technology, Rochester, NY, from 1976 to 1985. He was a Research Fellow at the Gordon Mckay Laboratory, Harvard University, Cambridge, MA, from 1977 to 1978. He is now a Professor in the Department of Electrical and Computer Engineering at Syracuse University. His current research interests deal with numerical solution of operator equations arising in electromagnetics and signal processing with application to system design. He has authored and coauthored over 154 journal articles and conference papers. He has written chapters in eight books.

Dr. Sarkar is a Registered Professional Engineer in the State of New York. He received the Best Paper Award of the IEEE Transactions on Electromagnetic Compatibility in 1979. He was an Associate Editor for feature articles of the IEEE Antennas and Propagation Society Newsletter. He was the Technical Program Chairman for the 1988 IEEE Antennas and Propagation Society International Symposium and URSI Radio Science Meeting. He is an Associate Editor for the IEEE Transactions on Electromagnetic Compatibility and for the *Journal of Electromagnetic Waves and Applications*. He has been appointed U.S. Research Council Representative to many URSI General Assemblies. He is also the Vice Chairman of the Intercommission Working Group of International URSI on Time Domain Meterology. He is a member of Sigma Xi and the International Union of Radio Science Commissions A and B. He also received one of the "best solution" awards in May 1977 at the Rome Air Development Center (RADC) Spectral Estimation Workshop.